scientific reports

OPEN

Comprehensive analysis of long-term trends, meteorological influences, and ozone formation sensitivity in the Jakarta Greater Area

Sheila Dewi Ayu Kusumaningtyas[1,2✉], Kenichi Tonokura[2✉], Robi Muharsyah[1], Dodo Gunawan[3], Ardhasena Sopaheluwakan[1], Windy Iriana[4,5], Puji Lestari[4], Didin Agustian Permadi[6], R. Rahmawati[7] & Nofi Azzah Rawaani Samputra[7]

Jakarta Greater Area (JGA) has encountered recurrent challenges of air pollution, notably, high ozone levels. We investigate the trends of surface ozone (O_3) changes from the air quality monitoring stations and resolve the contribution of meteorological drivers in urban Jakarta (2010–2019) and rural Bogor sites (2017–2019) using stepwise Multi Linear Regression. During 10 years of measurement, 41% of 1-h O_3 concentrations exceeded Indonesia's national threshold in Jakarta. In Bogor, 0.1% surpassed the threshold during 3 years of available data records. The monthly average of maximum daily 8-h average (MDA8) O_3 anomalies exhibited a downward trend at Jakarta sites while increasing at the rural site of Bogor. Meteorological and anthropogenic drivers contribute 30% and 70%, respectively, to the interannual O_3 anomalies in Jakarta. Ozone formation sensitivity with satellite demonstrates that a slight decrease in NO_2 and an increase in HCHO contributed to declining O_3 in Jakarta with 10 years average of HCHO to NO_2 ratio (FNR) of 3.7. Conversely, O_3 increases in rural areas with a higher FNR of 4.4, likely due to the contribution from the natural emission of O_3 precursors and the influence of meteorological factors that magnify the concentration.

Surface ozone (O_3), a secondary pollutant from complex photochemical reactions between precursors and sunlight, adversely affects human health and vegetation[1,2]. Changes in photochemical activity and meteorological parameters can alter surface O_3 concentrations[3–5]. Elevated temperatures and solar radiation accelerate the production of O_3[6]. Stagnant conditions and lower planetary boundary layers have also been linked with high O_3[7]. Surface O_3 formation is a nonlinear process involving nitrogen oxides (NO_x) and volatile organic compounds (VOCs) as precursors[8,9]. Thus, precursor emission changes can also modulate O_3 concentration in addition to meteorological factors. NO_x is primarily produced from anthropogenic sources, whereas VOCs arise from both natural (biogenic) and anthropogenic sources. O_3 sensitivity to the precursors depends on the photochemical regime of the O_3 formation[10]. Photochemical O_3 formation is influenced by a ratio of VOC to NO_x. The formation regimes are generally classified into VOC-limited regime (where O_3 formation is sensitive to an increase in VOCs), NO_x-limited regime (where O_3 concentration is mainly affected by an increase in NO_x and is insensitive to VOCs), and can be in a transitional state[4,11–13]. Understanding O_3 formation sensitivity is essential for establishing

[1]Agency for Meteorology, Climatology, and Geophysics of the Republic of Indonesia (BMKG), Jl. Angkasa I, No.2, Kemayoran, Jakarta 10720, Indonesia. [2]Department of Environment Systems, Graduate School of Frontier Sciences, The University of Tokyo, 5-1-5 Kashiwanoha, Kashiwa, Chiba 277-8563, Japan. [3]School of Meteorology, Climatology, and Geophysics (STMKG), Agency for Meteorology, Climatology, and Geophysics of Republic of Indonesia (BMKG), Pondok Betung, Tangerang Selatan, Indonesia. [4]Department of Environmental Engineering, Faculty of Civil and Environmental Engineering, Bandung Institute of Technology (ITB), Jl. Ganesa No. 10, Bandung 40132, Indonesia. [5]Center for Environmental Studies, Bandung Institute of Technology (ITB), Jl. Sangkuriang No.42 A, Bandung 40135, Indonesia. [6]Department of Environmental Engineering, Faculty of Civil Engineering and Planning, National Institute of Technology (ITENAS), Jl. PKH. Mustopha No.23, Bandung 40124, Indonesia. [7]Jakarta Provincial Environmental Agency, Jl. Mandala V No.67, RT.1/RW.2, Cililitan, Jakarta 13640, Indonesia. ✉email: sheila.dewi@bmkg.go.id; tonokura@k.u-tokyo.ac.jp

practical O_3 abatement efforts and remains a scientific challenge that must be addressed. Formaldehyde (HCHO) to nitrogen dioxide (NO_2) Ratio (FNR), derived from satellite measurements, serves as a valuable indicator for inferring O_3 formation due to its brief lifespan in the boundary layer and close association with O_3 formation[14–16]. Martin et al.[14] and Duncan et al.[15] combined satellite measurements and air quality models to establish the FNR threshold and concluded that FNR < 1 indicates a VOC-limited regime, FNR > 2 indicates a NOx-limited regime, and 1 > FNR > 2 indicates a transitional regime in the United States. Jin et al.[17] recently derived the FNR threshold for major U.S. cities with higher FNR values (3–4) in the transitional regime. In addition, Wang et al.[18] revealed that a VOC-limited regime occurs when FNR < 2.3, a NO_x-limited regime when FNR > 4.2, and an FNR between 2.3 and 4.2 reflects the transition regime in major Chinese cities.

Extensive research using modeling, ground measurements, and satellites has delved into surface O_3 trends and causes, and its formation sensitivity, yet Southeast Asia, particularly Indonesia, remains inadequately explored, as evidenced by limited studies[19–21]. The scarcity of O_3 measurements and a predominant focus on particulate matter reduction in Indonesia likely contribute to this research gap[22]. Indonesia currently installs 56 Air Quality Monitoring Stations (AQMS), twelve located in the Jakarta Greater Area (JGA). According to Verma et al.[23], considering the vast population of 273.8 million, the number of AQMS in Indonesia is still very few and requires 1039 more stations. JGA is Indonesia's largest urban agglomeration, comprising Jakarta's capital and satellite cities such as Bogor, Depok, Bekasi, and Tangerang. The JGA has a dense population, rapid economic development, intensive industrialization, and high transportation utility. Bogor, located in the southern part of Jakarta, encompasses an area five times larger than that of Jakarta. With distinctive topography, Bogor functions as a downwind location influenced by local and transported emissions. An air quality station in Cibeureum (CBR), southeast Bogor, reflects a background environment close to Jakarta's.

This article unveils the seasonal variations and temporal trends in O_3 concentrations within urban Jakarta and rural Bogor employing ozone metrics. The investigation assesses the contribution of meteorological and anthropogenic factors to O_3 changes utilizing stepwise Multiple Linear Regression (MLR). Furthermore, the study analyzes O_3 formation sensitivity using FNR derived from satellite observations and compares them with the previous studies. This study extends beyond Jakarta, offering insights with broader implications for other megalopolitan areas grappling with similar environmental challenges.

Results

Seasonal variation and temporal trends of ozone (O_3)

Figure 1 depicts the time series of maximum daily 8-h average (MDA8) monthly anomalies and the trends in the 10th, 50th, and 90th percentiles at five sites in urban Jakarta (hereinafter refers to DKI) and one rural site of CBR. All DKI sites generally exhibit a downward trend of surface O_3 in the 50th percentile, as presented in
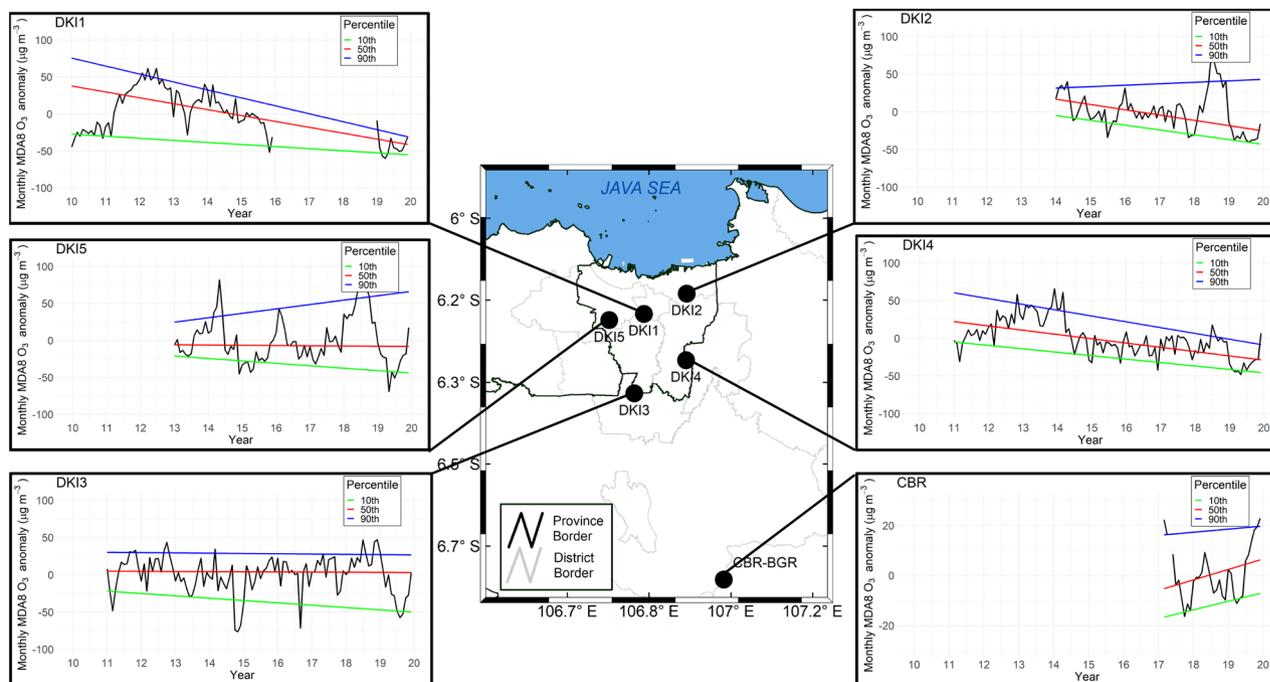

Figure 1. Map of the study area and the time series of the monthly mean anomaly of ozone maximum daily 8-h average (MDA8 O_3) during the study period at Jakarta and Bogor sites. Color solid lines denote linear trends in the 90th (blue), 50th (red), and 10th (green) percentiles. Pink shade represents Jakarta Province with sites in central Jakarta (DKI1), north (DKI2), south (DKI3), east (DKI4), and west (DKI5). CBR represents the site in rural Bogor. The shapefile for Jakarta Greater Area boundary map is obtained from Geospatial Information Agency of Indonesia https://geoservices.big.go.id/petarbi/ and the map plot is generated using ArcGIS Pro online 2.8.0. The plot graph is generated using RStudio 1.4.1106. 2021.

Table 1. Highest O_3 declining rate occurs in DKI1, DKI2, DKI4, DKI5, and DKI3 by about -8.0 μg m^{-3} year^{-1}, -7.1 μg m^{-3} year^{-1}, -5.7 μg m^{-3} year^{-1}, -0.3 μg m^{-3} year^{-1}, and -0.2 μg m^{-3} year^{-1}, respectively. The tenth percentile represents low O_3 concentration that may not involve or is less involved in photochemical reaction[24]. DKI2 in northern Jakarta appeared to have the highest and significant declining rate of -6.4 m^{-3} year^{-1} for the 10th percentile, followed by DKI4 (-4.6 μg m^{-3} year^{-1}), DKI5 (-3.3 μg m^{-3} year^{-1}), DKI3 (-3.1 μg m^{-3} year^{-1}), and DKI1 (-2.8 μg m^{-3} year^{-1}).

Meanwhile, MDA8 O_3 anomaly trends in the 90th percentile show different directions from one site to another. Central (DKI1), south (DKI3), and east (DKI4) Jakarta shows a decreasing trend in different order of magnitude. DKI1 and DKI4 experience faster concentration decreases and significant rates of -10.7 μg m^{-3} year^{-1} and -7.7 μg m^{-3} year^{-1}. DKI1 and DKI4 perform at faster-decreasing rates than their lower (50th and 10th) percentiles, indicating reduced extreme ozone episodes during the study period. Despite the reduction rate of O_3 in the 50th and 10th percentiles, DKI2 and DKI5 present insignificant upward trends in the 90th percentile with a rate of 1.9 μg m^{-3} year^{-1} and 5.9 μg m^{-3} year^{-1}, respectively, suggesting increase number of extreme O_3 concentration.

The MDA8 O_3 (average from all DKI sites) exceedance frequency (>100 μg m^{-3} for 8-h threshold) in the dry season showed a sharp rise after 2010, fluctuated until 2018, but underwent a remarkable reduction in 2019, as demonstrated in Supplementary Fig. S1a. The minimum (maximum) exceedance frequency was observed in 2019 (2012). A yearly average of MDA8 O_3 concentration surpassing the 8-h threshold, calculated from daily data, shows a slight reduction from 2011 to 2019 (see Supplementary Fig. S1b). This finding corresponds with the significant downward trend in high O_3 concentration (90th percentile) observed at specific DKI sites, as depicted in Fig. 1 and Table 1.

The MDA8 O_3 increased during the dry period across DKI and CBR sites, peaking in October. Figure 2 displays a map of the average maximum daily 8-h of ozone (AVGMDA8) in urban Jakarta and rural Bogor during the study period for the dry season (April to November). The AVGMDA8 varied and showed consistency with the 1-h O_3 value, with the highest concentration at DKI3, followed by DKI5, DKI2, DKI4, and DKI1 with values of 128, 127, 122, 111, and 99 μg m^{-3}, respectively. During 10-year period from 2010 to 2019, all DKI sites

Site	90th percentile	50th percentile	10th percentile
DKI1	**−10.7 ($p = 0.00072$)**	−8.0	−2.8
DKI2	1.9	−7.1	**−6.4 ($p = 0.00017$)**
DKI3	−0.4	−0.2	−3.1
DKI4	**−7.7 ($p = 0.000015$)**	**−5.7 ($p = 0.0038$)**	**−4.6 ($p = 0.00012$)**
DKI5	5.9	−0.3	−3.3
CBR_BGR	1.3	4.2	3.4

Table 1. Slope values from QR annual trend analysis for different percentiles at DKI (2010–2019) and CBR sites (2017–2019). Bold indicates 95% significance two-tailed test reached.
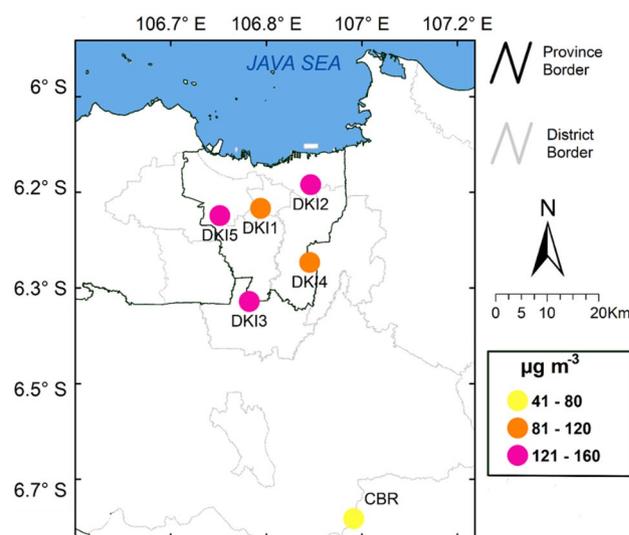

Figure 2. Map of the average of Maximum Daily 8-h ozone (AVGMDA8) in urban (Jakarta) and rural (Bogor) during the dry season (April to November) over the entire study period. (ArcGIS Online Pro 2.8.0. 2021). The shapefile for Jakarta Greater Area boundary map is obtained from Geospatial Information Agency of Indonesia https://geoservices.big.go.id/petarbi/ and the map plot is generated using ArcGIS Pro online 2.8.0.

exceeded the National Ambient Air Quality Standard (NAAQS) for 1-h concentration of O_3 (1-h O_3 >150 µg m^{-3}) with 18%, 26%, 30%, 37%, and 41% of exceedances, respectively, at DKI1, DKI4, DKI2, DKI3, and DKI5, as presented in Supplementary Fig. S2. The CBR experienced the 1-h O_3 concentration threshold exceedances of 0.1% during 2017 to 2019. The monthly variations in 1-h O_3 at the DKI and CBR sites peaked between May and November with an upward trend. The O_3 concentrations gradually decreased from December to April. During the observation period, DKI5 experienced the highest annual average of 1-h O_3 concentration compared to other sites with a maximum (minimum) of 194 µg m^{-3} (97 µg m^{-3}), followed by DKI2 and DKI3, which were 160 µg m^{-3} (107 µg m^{-3}) and 147 µg m^{-3} (103 µg m^{-3}), respectively.

The overall O_3 level at the CBR site was considered low compared to that in DKI sites and the NAAQS; however, the annual 1-h and MDA8 values increased from 2017 to 2019. MDA8 O_3 anomaly increased in all percentiles by approximately 1.3 µg m^{-3} year^{-1} (90th), 4.2 µg m^{-3} year^{-1} (50th), and 3.4 µg m^{-3} year^{-1} (10th), indicating the enhanced presence of precursors that have critical roles in photochemical O_3 formation in this area. Changing O_3 concentration in the 10th percentile represents changes in the local background of O_3 concentration[24].

Meteorological impact on the MDA8 O_3 variation

The MLR model yielded the adjusted coefficients of determination (R^2) for Jakarta (average from five DKI sites) and CBR areas for all seasons of 0.28 and 0.43, respectively, implying that 28% and 43% of the MDA8 O_3 daily variability were associated with meteorological conditions. The contributions of meteorological and anthropogenic factors to the monthly mean MDA8 O_3 anomalies in Jakarta and CBR areas over the entire period are depicted in Fig. 3a,b, respectively. Meteorological components influenced inter-annual O_3 changes in Jakarta, accounting for 30% of the relative contribution for the entire season of 2013–2019. In general, meteorological components contribution ranged from 0.2 to 98.5% and was not considerably different from that of the dry season (Supplementary Fig. S3a). A slightly lesser meteorological influence shows during the wet season with a 25% relative contribution to O_3 variability.
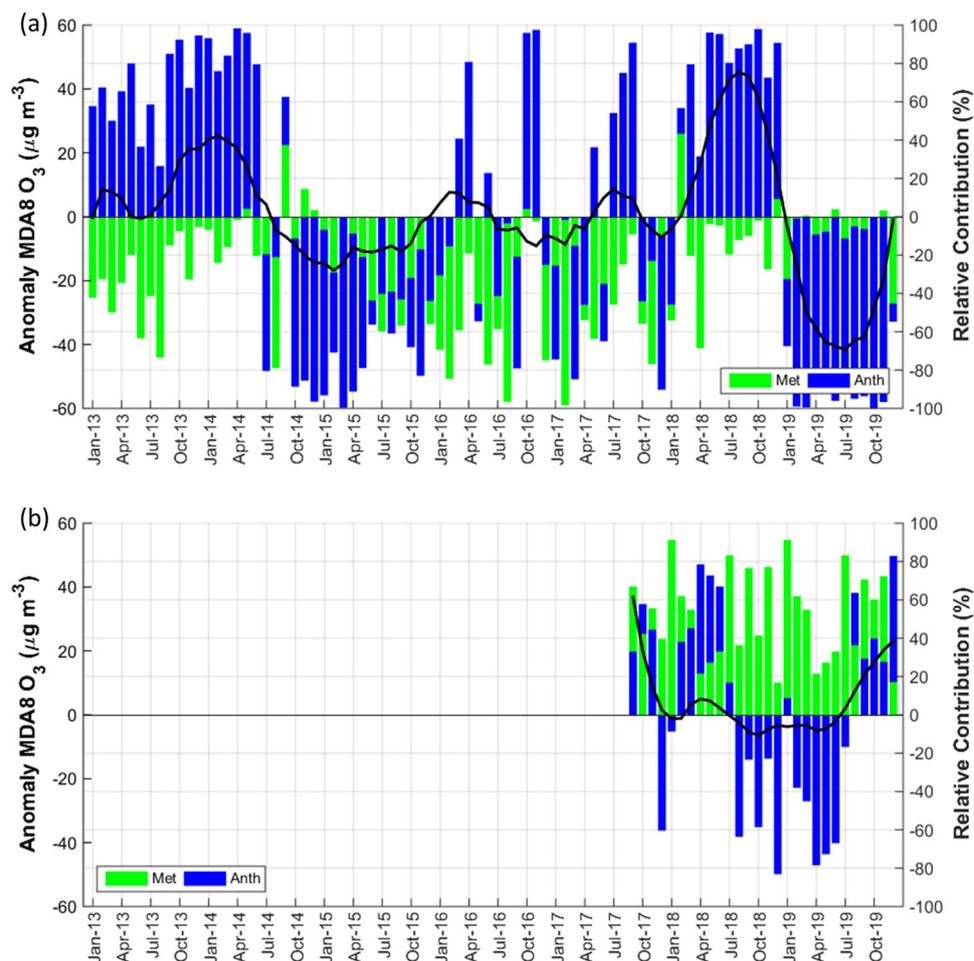

Figure 3. Contribution of meteorological (green bar) and anthropogenic factor (blue bar) to observed MDA8 O_3 anomalies (black line) in (**a**) Jakarta (2013–2019) and (**b**) Bogor (2017–2019). (Matlab R2014b, 2014. 416,517).

Pronounced positive contributions from meteorological features such as February 2018 altered MDA8$_{obs}$ very slightly. Anthropogenic factors contributed 70% to the inter-annual variability of ΔMDA8$_{obs}$, averaging 1.5–99.8%. Notably, positive ΔMDA8$_{obs}$ in 2013, half of 2014, and 2018 were primarily attributed to anthropogenic rather than meteorological. The positive anthropogenic contribution reached more than 90% and was responsible for the increase of monthly mean ΔMDA8$_{obs}$ during those years. The monthly mean of ΔMDA8$_{obs}$ fluctuated and increased significantly in 2018 (Fig. 3a). These results indicate that changes in anthropogenic emissions are more favorable for O$_3$ production, particularly during the dry season.

Downward UV radiation at the surface (UVB) significantly contributed to the O$_3$ variation in all seasons, although the coefficient was minimal (Table 2). UVB also revealed a positive correlation with the correlation coefficient of $r = 0.32$, the second-highest value after wind speed (Supplementary Table S2). The UVB pattern was synchronous with maximum temperature (Tmax), particularly during the dry season, as shown in Supplementary Fig. S4c,d. Intense UV radiation is favorable for ozone production. Furthermore, higher temperatures can increase HCHO concentrations from biogenic emissions[25]. More than 70% of the daily observed MDA8 was above the NAAQS and coincided with UVB > 70,000 J m^{-2}. According to Indonesian Meteorological Office (BMKG), the UV index in Jakarta at 10:00 local time was estimated to be 2–6, indicating a moderate to high risk. A negative anomaly of UVB influenced the O$_3$ decline in 2013 (-8.5 µg m^{-3}) (Supplementary Fig. S4d). However, the high negative anomaly of UVB in 2016 (-7759 J m^{-2}) was likely canceled out by the positive contribution of Relative Humidity (RH), thus inducing only a small perturbation in O$_3$.

UVB and wind speed mean (WS_MEAN) showed higher correlations than other parameters in Jakarta. The wind speed significantly ($p = 2 \times 10^{-16}$) contributed to the stepwise MLR. Wind speed is negatively correlated with MDA8 O$_3$. During the dry period, air stagnation frequently occurred in Jakarta, boundary layer height (BLH) was low, calm winds dominated and recorded as approximately 70% of prevailing winds, and the wind speed was < 3 m s^{-1} leading to pollutant accumulation on the surface[26,27]. There is likely a contribution from the significant negative anomalies of the mean wind speed in 2018 (-0.2 m s^{-1}) to the increased MDA8$_{met}$ (5.9 µg m^{-3}) during the dry period (in Supplementary Fig. S3a). The BLH contributed negatively to Jakarta's MDA8 O$_3$ change, indicating that shallow BLH increases O$_3$ concentration. In addition, the immense positive contribution from emission drivers in 2018 substantially influenced the overall increase in O$_3$ levels at the DKI sites. High RH is associated with enhanced cloud cover and a greater chance of rainfall, slowing the photochemical reaction of ozone formation[3,4].

Meteorological and anthropogenic components shared almost equal proportions over 3 years' period of measurement from 2017 to 2019 at CBR site, with average proportions of 52% (ranging from 17 to 91%) and 48% (ranging from 9 to 83%), respectively. However, the number did not change significantly during the dry season. UVB ($p = 3 \times 10^{-6}$), BLH ($p < 2 \times 10^{-16}$), Tmax ($p = 0.005$), and Surface Pressure (SP) ($p = 1.7 \times 10^{-6}$) significantly contributed to O$_3$ variation at CBR. The CBR site exhibits complex terrain and thus presents unique weather conditions. High-altitude areas experience lower pressure. With a forced inversion layer and slow wind speeds, vertical mixing and horizontal dispersion in the atmosphere are poor and hindered by mountains, leading to increased concentrations of pollutants[28]. BLH was significant in CBR and had moderate positive correlations. In higher-altitude areas, during the development of a boundary layer, intrusion of O$_3$ from the upper atmosphere to near the surface is possible, thus contributing to the surface O$_3$ level[29,30]. This could be a possible reason for a positive correlation between BLH and O$_3$ concentration. A similar characteristic of BLH and O$_3$ variations observed at the CBR site is also evident in other locations with comparable geographic features. For instance, Mount Lulin in Taiwan[31] and certain sites in in Beijing-Tianjin-Hebei Province and the Yangtze River Delta, China[4].

Spatial and temporal analysis of OMI NO$_2$ and HCHO column density

The NO$_2$ monthly average in Jakarta ranged from 1.5 to 8.5 × 10^{15} molecules cm^{-2}, with a 10-year average of 3.6 × 10^{15} molecules cm^{-2} (Fig. 5a). This value is lower than those of cities in Japan[13], China[9,11], London[32], and Mexico city[12] for the same study period. The trend in the 50th percentile depicted an insignificant downward trend, with rates of -0.04×10^{15} and -0.01×10^{15} molecule cm^{-2} year^{-1} in Jakarta and CBR, respectively. The tropospheric NO$_2$ in CBR is lower than in Jakarta, with a 10-year average of 2.9 × 10^{15} molecule cm^{-2} and ranging from 1.1 to

	Variable	Jakarta (2013–2019)			CBR (2017–2019)		
		All seasons	Dry season	Wet season	All seasons	Dry season	Wet season
Selected variable	WS_MEAN	− 22	− 24.72	− 4.98	− 5.93	3.98	
	UVB	0.00034	0.000514	0.00051	0.00023	0.00037	0.0003278
	TMAX	4.77	2.71	3.60	1.66	− 1.41	1.18
	RH	− 0.695	− 0.372	− 0.954	0.36		0.713
	BLH	− 0.010	− 0.016	− 0.0908	0.082	0.064	− 0.0404
	SP	− 0.0149	− 0.01	− 0.0378	0.0238	0.00125	
Intercept		1516	948	3700	− 2329	− 1156	− 0.74
R^2		0.28	0.20	0.30	0.43	0.47	0.16

Table 2. Coefficient of several variables from the multiple linear regression (MLR) model results for Jakarta (2013–2019) and CBR sites (2017–2019) in the dry, wet, and all seasons. *P* value coefficient is presented in Supplementary Table S3.

5.5×10^{15} molecule cm^{-2}. Although the trend slightly decreased, a substantial increase was observed in the NO_2 OMI from 2017 to 2019, with a slope of 0.02×10^{15} molecules cm^{-2} $month^{-1}$.

HCHO column density presented an insignificant upward trend of 0.19×10^{15} (0.23×10^{15}) molecule cm^{-2} in Jakarta (CBR). 10-year average of OMI HCHO column density in urban Jakarta was 12.6×10^{15} molecules cm^{-2} with monthly average ranging from 0.9 to 19.4×10^{15} molecules cm^{-2} (Figs. 4a and 5b). This number is greater than that of urban areas in China (~2 to 18×10^{15} molecules cm^{-2} in Beijing and Shanghai), Japan (~1 to 16×10^{15} molecules cm^{-2} in Tokyo, Osaka, and Nagoya), and Mexico City (~3 to 9×10^{15} molecules cm^{-2})[12,33].

OMI HCHO in CBR area is lower than in Jakarta, with a yearly average of 10.9×10^{15} molecules cm^{-2} over the entire study period (Fig. 5b). Biogenic VOC emissions from plants and vegetation are more reactive than anthropogenic VOCs, causing relatively high HCHO columns over cropland areas such as CBR. However, anthropogenic Non-Methane VOC (NMVOC) emissions surpass biogenic VOC emissions[11] in urban cities where anthropogenic activities are massive and intense. Anthropogenic NMVOC emissions in Bogor from on-road motorized vehicles was around 9.7 Gg $year^{-1}$ in 2016[34], one-fifth smaller than Jakarta's emission for the same sector (48.6 Gg $year^{-1}$ in 2015)[35].

Seasonal variation of OMI NO_2 and HCHO

Seasonal variations in NO_2 concentrations in Jakarta and CBR exhibited the same pattern, increasing in April and gradually decreasing in October. In Jakarta, the maximum (minimum) NO_2 concentration occurred during the dry (wet) period in July (December) (Fig. 5d,g, and Supplementary Fig. S7). Enhanced column density occurred in northern Jakarta and extended to Bogor city center during the dry period (Fig. 5d). We also examine the monthly variability of NO_2 from in-situ measurements and reveal that the concentration fluctuates throughout the year, and the seasonal pattern is not too obvious, as depicted in Supplementary Fig. S7. Sofyan et al.[36] found no significant differences in fuel consumption in Jakarta between the dry and wet seasons. However, there is an apparent effect of sea breeze on transporting NO_2 from north Jakarta to central and southern Jakarta. On dry
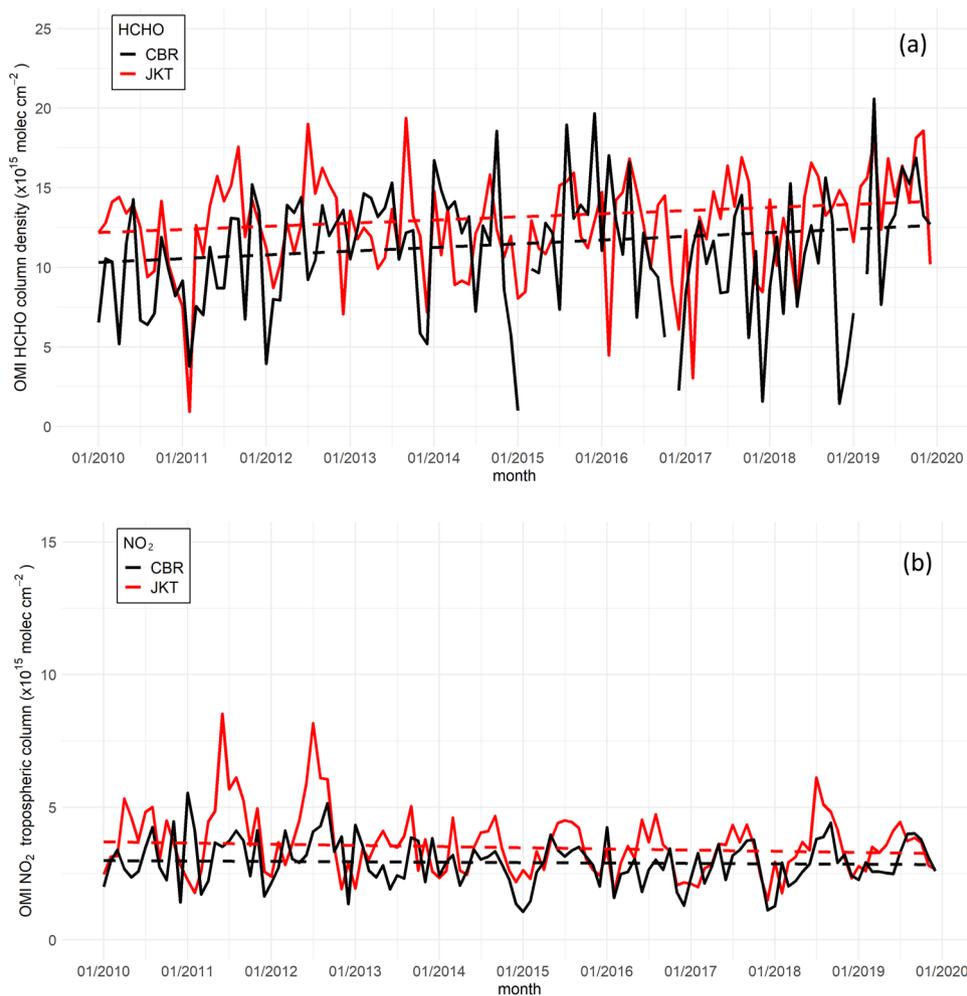

Figure 4. Monthly average of (**a**) HCHO column density and (**b**) NO_2 tropospheric column from 2010–2019 in Jakarta and Cibeureum Bogor. The dashed line represents a trend in the 50th percentile. (RStudio 1.4.1106. 2021).
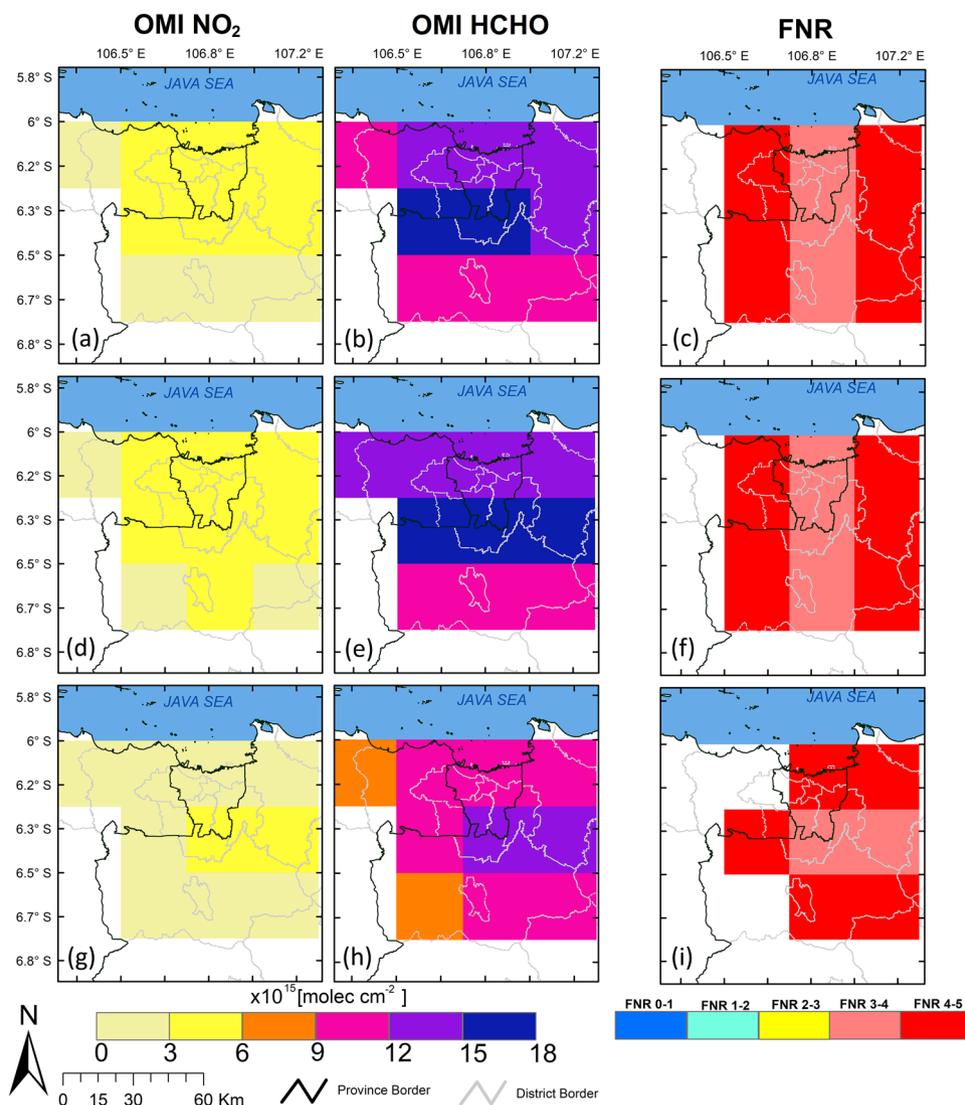
Figure 5. Map of the average (**a**) OMI NO$_2$ tropospheric column, (**b**) OMI HCHO vertical column, and (**c**) FNR value from 2010–2019 for all seasons; (**d**), (**e**), and (**f**) for dry seasons; and (**g**), (**h**), and (**i**) for the wet season. Transparent areas indicate an FNR value above 5. The shapefile for Jakarta Greater Area boundary map is obtained from Geospatial Information Agency of Indonesia https://geoservices.big.go.id/petarbi/ and the map plot is generated using ArcGIS Pro online 2.8.0.

days, converging sea breezes in the southern part of Jakarta cause pollutant accumulation in central Jakarta[36]. The pollutants then move along the sea breeze front and penetrate the Bogor area.

Generally, NO$_2$ in Jakarta was higher than in CBR for the whole seasons. The maximum NO$_2$ concentration in CBR occurred in September, and the minimum in December. The reduction in NO$_2$ was mainly due to meteorological conditions during the wet period. Disregarding exceptional circumstances such as movement restrictions during the COVID-19 pandemic, which were not considered in this study, anthropogenic emissions in Jakarta and CBR were steady throughout the year.

Compared to NO$_2$, HCHO was higher during the dry than wet period but fluctuated more (Fig. 5e,h). A slightly higher temperature during the dry period accelerated VOC photochemical oxidation, thereby contributing to high levels of HCHO. Elevated HCHO levels were notable and extended northwest and northeast of Jakarta during the dry period from 2010 to 2019, as shown in Fig. 5e. The HCHO column density in the whole Bogor area varied significantly seasonally. However, it was slightly lower in northwestern Bogor than in central Bogor.

OMI FNR

Figure 5c presents the spatial yearly average FNR value from 2010 to 2019 in JGA. FNR in Jakarta steadily increased to 4.5, consistent with the increase in HCHO column density (Fig. 4a). Seasonal variations in the FNR occurred in Jakarta and CBR (Fig. 5f,i, and Supplementary Fig. S9b). As expected, the FNR decreased in Jakarta's

dry period but fluctuated slightly in CBR. The reduction in FNR during the dry period was consistent with that shown in Supplementary Fig. S7, where the NO_2 tropospheric column increased.

During the dry period, the maximum 1-h O_3 and MDA8 O_3 showed more days exceeding the 1-h and 8-h NAAQS thresholds than the wet period. It is worth noting that a large positive MDA8 O_3 anomaly in 2018 was mainly driven by a large positive anomaly in anthropogenic activity. The increased MDA8 O_3 is likely due to a response from the increase of OMI NO_2 under a high FNR value of 3.9. However, to confirm this finding, further modeling work should be conducted.

Discussion

O_3 concentration and its formation mechanism are influenced by meteorology and changes in VOC and NO_x. The O_3 formation sensitivity could be either VOC-sensitive, NO_X-sensitive, or transitional, where an increase of both precursors affects the O_3 production. In a vibrant urban agglomeration such as JGA, characterized by intense emissions and limited and scattered AQMS, investigating the long-term trends of O_3 pollutants and their formation regimes becomes imperative for effective air quality management. Identification of O_3 formation sensitivity aids policymakers in designing appropriate control strategies. The current study evaluates trend and meteorological influences on O_3 concentration variability. Additionally, we leverage space-borne NO_2 and HCHO tropospheric column density to compute FNR as a VOC/NO_X ratio proxy to characterize O_3 formation regimes.

Generally, our results show a downward trend of MDA8 O_3 anomalies at all sites except CBR of rural Bogor. Despite the reduction trend, some sites experienced an increasing trend of high O_3 episodes, such as in northern and western Jakarta, and almost steady state in southern Jakarta. This feature leads to high episodes exceeding the national standard for 1-h and 8-h O_3 concentration from 2010 to 2019. As much as 41% of 1-h O_3 concentration exceeded the national threshold for the whole seasons from 2010 to 2019 and 93% for MDA8 O_3 in the 2018 dry season for Jakarta, with annual averages reaching 158.9 µg m^{-3}. It is worth noting that high positive anomalies of O_3 during 2018 are influenced mainly by anthropogenic drivers rather than the meteorology, as can be seen in Fig. 3a. It is likely due to a response from the increase of OMI NO_2 under increase FNR value of 3.9 (Fig. 4b). However, to confirm this finding, further modeling work should be conducted.

DKI1 is in the city center, while DKI2 is near the busy harbor, power plants, and industrial areas. Both sites are characterized by higher NO_X emissions owing to high anthropogenic activities, as reflected by higher NO_2 concentration (see Supplementary Fig. S8). In the vicinity of high NO emissions, O_3 is removed via NO titration. However, its concentration increases further downstream, as in DKI3 and DKI5. DKI3 and DKI5 presented higher exceedance episodes and the least declining O_3 trend. During the dry period, wind direction toward Jakarta mainly originated from the east and southeast, allowing the transport of pollutants from outside Jakarta to the eastern part of Jakarta, where industrial and manufacturing centers are located (around the Bekasi industrial area), contributing to the increase in O_3 concentration at DKI5 (western Jakarta). In July, the HYbrid Single-Particle Lagrangian Integrated Trajectory (HYSPLIT) model's backward trajectory showed that air mass transport originated from Karawang and passed through Bekasi and South Jakarta (Supplementary Fig. S10). Despite the synoptic scale of easterly and southeasterly winds during the dry season, Jakarta was affected by sea breezes. According to Kitada et al.[37], the southerly land breeze carried pollutant-rich but ozone-poor air masses to the Jakarta coast at night. In the morning, photochemical reactions produce O_3 in northern Jakarta, and sea breeze circulation develops in the lower layers under weak synoptic winds[37]. The sea breeze, opposite the easterly and southeasterly winds, became dominant owing to the easterly and southeasterly synoptic scales blocked below approximately 1 km by the mountains in the southern part of West Java. The O_3-rich air mass was transported to southern Jakarta and Bogor as the sea breeze propagated inland up to 60 km from the Jakarta coastline[37,38]. This sea breeze phenomenon affects the convection activity and transport of atmospheric pollutants, which explains the high concentration of DKI3 downwind of Jakarta.

Measurement of OMI NO_2 in Jakarta shows an insignificant decreasing trend and increasing HCHO from time to time. In metropolitan cities in the US, China, Mexico, and Japan, tropospheric NO_2 outnumbers the HCHO. Thus, the O_3 formation is VOC-limited regime, as shown in Table S5. However, that is not the case for Jakarta, where HCHO column leads. As a consequence, the FNR falls in higher value compared to those cities. Study from Lestari et al.[35] shows that the most significant emission load was from CO, NO_X, and NMVOC, at approximately 52.9, 143.9, and 48.6 kilotonnes in 2015, respectively. Significant contributors to NO_X were the road transportation sector (57%), power plants (24%), industrial sectors (15%), and residential areas (4%)[35,39,40]. Furthermore, by Lestari et al.[35], the total emissions inventory of NMVOC in Jakarta was comparable to that of NO_X in the same sectors and years. Road transport was the major contributor to NMVOC in Jakarta, with a percentage of 96%, followed by industry at 2%, power plants and residential areas at 1%. According to the Ministry of Transportation of the Republic of Indonesia, there was a total transportation movement of 19.63 million movements/day in 2022. Road transport by motorcycles contributed to 88% of the total NMVOC emissions. Jakarta Provincial Agency documented that there were over 15.8 million motorcycles in the city in 2019, approximately a 2.7% increase from 2018. Motorcycles represent the dominant vehicle fleet in Jakarta Province, accounting for approximately 80% of the total vehicles, followed by cars (17%), trucks (3%), and buses (0.2%)[41]. Similar emission types were also found in Vietnam, where motorcycles mainly contributed to the VOC emissions in Hanoi and Ho Chi Minh City. Motorcycles comprise 80% of the total transportation in Vietnam, and the number of vehicles per 1000 population in Vietnam is lower than that in Jakarta[42,43]. Emissions from motorcycles are likely attributable to high HCHO column density in Jakarta. In addition, NMVOCs are abundant in certain areas, such as gas stations[44] and solvent usage industries[45].

Different features occurred at the rural CBR site. A 3-year measurement period shows that the O_3 concentration is below the government threshold; however, it shows an increasing rate for all percentiles. The growing O_3 concentration value at the rural site indicates the enhanced presence of precursors that have critical

roles in photochemical O_3 formation. Changes in O_3 concentration in the 10th percentile represent changes in the local background of O_3 concentration. Unlike Bogor, a decreasing trend in O_3 was observed in the rural North China Plain, Europe, and North America, likely because of the implementation of the O_3 control policy[24].

Bogor has a lower population density and more vegetation than Jakarta. The number of vehicles in Bogor is two million, one-thirteenth of those in Jakarta (26 million)[41]. Bogor, as the outskirt of Jakarta, may receive pollutants transported from Jakarta along with the sea breeze; however, this may not contribute substantially to the total emissions of the CBR. Lower concentrations recorded at the CBR were expected owing to lower emission activity, local characteristics, and meteorological disparity.

Air pollution prevention policies have been implemented in Indonesia and locally in JGA for more than a decade. For example, national kerosene-to-LPG conversion for cooking has been proven to reduce emissions[40]. Decreasing particulate matter, sulfate, and nitrate concentrations in Jakarta since 2006 have been used as evidence for the successful implementation of national and local policies, such as Regulation No. 141 concerning the Utilization of Gas Fuel for Public Transportation and Local Government Operational Vehicles[46]. Another successful implementation policy was issuing the Ministry of Environment and Forestry decree number 20/2017 on the usage of EURO IV for gasoline vehicles in late 2018. One current policy is that of the Governor of the DKI Jakarta, Regulation No. 66/2020 on vehicle emission testing, which regulates penalties for vehicles that violate the regulations.

Despite its ongoing implementation of measures, O_3 pollution episodes persist. A more aggressive NO_X reduction should be in place in Jakarta. Thorough investigations of the precursors and emission inventory calculation are essential to enhance our understanding of O_3 formation. Moreover, the thresholds for regime classification in Jakarta may require adjustment compared to global FNR thresholds. Further researches, combining modeling and observations, are warranted to identify effective O_3 reduction scenarios for informed policy recommendations.

Summary and conclusion

This study investigated variations and temporal trends in surface O_3 under two different background conditions: urban (Jakarta, 2010–2019) and rural (Bogor, 2017–2019). We assessed the contributions of meteorological and anthropogenic factors and the long-term O_3 formation sensitivity derived from OMI measurements. Despite the downward trend of O_3 anomalies attributed to a slight reduction of NO_2 concentration, Jakarta experiences recurrent elevated O_3 level surpassing both the 1-h and 8-h national thresholds. Generally, anthropogenic drivers are more dominant than meteorological, irrespective of seasonal variations. However, O_3 pollution can be even more severe under changing climate. Further research will focus in modeling simulations to validate the O_3 sensitivity findings presented in this paper and eventually to establish O_3 chemical regime thresholds, which are crucial for devising effective strategies to mitigate O_3 pollution in JGA.

Data description and methodology
Study sites and air quality data

Jakarta, the center of government, business, and economic activities, contributes the most to the national gross domestic product with over 190 million USD in 2019[47]. We used air quality data from five AQMS in Jakarta (2010–2019) operated by the Environmental Agency of Jakarta Province, one station in Cibeureum Bogor (2017–2019) operated by the Meteorological, Climatological, and Geophysical Agency (BMKG) in collaboration with the National Institute of Environmental Studies (NIES), Japan, as presented in Fig. 1 and Supplementary Table S1. Further local characteristics of Jakarta and Bogor are described in Supplementary Table S6. We used hourly O_3 concentrations and preprocessed the data to eliminate negative values and outliers. The time series of the hourly concentrations were normalized using the z-score following the methodology used by Ren et al. and Sun et al.[24,48]. Points with an absolute z-score greater than 4 ($|zt| > 4$) were removed from the time series. The daily average was calculated when a station had more than 60% hourly data, and we considered daily data missing if the availability was below this threshold.

Surface O_3 measurement

Jakarta Environmental Agency continuously measures 30-min surface O_3 using HORIBA APOA-370 analyzer. The APOA-370 continuously monitors atmospheric ozone concentrations using a cross flow modulated ultraviolet absorption method or Non-dispersive ultraviolet absorption (NDUV). The NDUV measures ozone O_3 concentration in sample gases using UV light absorption. UV light is emitted into a gas cell where the sample gas flows, and O_3 absorbs UV light proportionally to its concentration. The absorbed light is detected by a photodiode, generating electrical signals. NDUV employs a cross-modulation method with a solenoid valve unit to switch between sample and reference gases, allowing the detector to distinguish AC and DC signals during processing. AC signals represent gas concentration, while DC signals compensate for UV light source aging, ensuring analyzer stability. CBR site in collaboration with NIES measure O_3 concentration continuously using Kimoto OA-787[49].

Meteorological data

Meteorological data were used to construct the stepwise MLR model. Parameters such as Tmax, rainfall (RRR), WS_mean, and RH of Jakarta and Bogor were obtained from the BMKG. Other meteorological parameters, such as the BLH, SP, and UVB, were downloaded from the European Center for Medium-Range Weather Forecasts Reanalysis (ECMWF ERA5) product on single levels with a spatial resolution of 0.25° × 0.25° and a temporal resolution of 1 h for the corresponding grid, similar to the meteorological stations and AQMS (https://cds.climate.copernicus.eu/cdsapp#;/dataset/).

Satellite product

We use level three gridded data of the daily ozone-monitoring instrument (OMI)[50] NO_2 tropospheric column standard product (OMNO2d_003) with a cloud fraction of less than 30% and a spatial resolution of 0.25°×0.25° downloaded from https://disc.gsfc.nasa.gov/. To calculate the ratio, we average the NO_2 daily data to monthly. The monthly level three vertical column density of OMI HCHO was downloaded from the European Quality Assurance for Essential Climate Variables project (QA4ECV) (http://www.qa4ecv.eu) with a spatial resolution of 0.05°×0.05°. The QA4ECV HCHO slant column densities (SCDs) have 8–12×10^{15} molecule cm^{−2} uncertainties. We re-grid the monthly OMI HCHO data to 0.25°×0.25° to match the monthly OMI NO_2 data.

Trend analysis of ozone metrics

To identify O_3 pollution, we use an indicator from the Indonesian Government Regulation No. 22 Year 2021 on the implementation of environmental protection and management for 1-h O_3 concentration (measured from 11:00 to 14:00 local time) and O_3 metric following the Tropospheric Ozone Assessment Report (TOAR), such as the maximum daily 8-h average (MDA8)[51]. This metric is intended to evaluate the impact of O_3 on human health, vegetation, model comparisons, and the characterization of O_3 in the free troposphere[51]. MDA8 O_3 was calculated from 24 running 8-h averages. The 8-h running mean for a particular hour is computed based on the concentration for that hour plus the following 7 h. The daily maximum 8-h concentration for a given calendar day was the highest of the 8-h average concentrations computed for 8-h periods starting from that day. The 8-h running mean was considered valid when at least 5 h of data were available (60% completeness was required). The average MDA8 (AVGMDA8) is the mean value of daily MDA8 (calculated based on more than 60% of the daily MDA8).

Quantile Regression (QR) estimates the trend in MDA8 O_3 concentration. QR is a well-suited technique for detecting heterogeneous distributional changes, which is often the case for free tropospheric and surface ozone as they typically show diverse percentile trends[52]. Trend uncertainty is estimated by doing a moving block bootstrap algorithm to take autocorrelation into account in the trend uncertainty. Trend analysis considers the seasonality of MDA8 O_3 time series by calculating the MDA8 O_3 anomaly. MDA8 monthly anomalies are more accurate than the monthly average in case of missing data[10,48,53]. Monthly anomalies were calculated by subtracting the individual monthly mean from the monthly mean for the same month for the entire study period. Meanwhile, zero anomaly refers to a situation where the monthly MDA8 O_3 is equal to the long-term average value or no deviation or departure from the average conditions. QR analysis is computed using Rstudio with a quantreg package.

Stepwise multiple linear regression (MLR) model

Statistical models were used to infer the contributions of meteorological and anthropogenic factors to the monthly ozone variability. Researchers commonly use the MLR to quantify the effects of meteorological factors on O_3[4,6,9,10,24]. The MLR uses the following equation to reflect the relationship between a quantitative dependent variable and two or more independent variables:

$$y_{s,c} = \beta_o + \sum_{k=1}^{n} \beta_{s,c} x Met_k + \varepsilon \tag{1}$$

The stepwise MLR estimated MDA8 O_3 from meteorological factors (MDA8_{met}); where y is the daily observed MDA8 O_3 (MDA8_{obs}) in season s (dry, wet, and all seasons) and city c (Jakarta and Bogor); Met_k is the selected daily meteorological parameter; $\beta_{s,c}$ is the regression coefficient in season s and city c; β_o is the intercept; and ε is the residual. MDA8_{obs} used to construct the model were averaged from the MDA8_{obs} at five sites in Jakarta and one for rural Bogor.

A series of steps was conducted to determine the relative meteorology contribution to O_3 variation. First, correlation coefficients were established between MDA8_{obs} and all meteorological parameters (see Supplementary Table S2). Second, the Variance Inflation Factor (VIF) was calculated to avoid multicollinearity between variables. Variables with a VIF > 10 indicated multicollinearity removal, and those with a 10 were retained. In this study, all the predictors had a VIF < 10 (approximately 1–3) and were retained for the next selection step. Third, stepwise regression was conducted to obtain the best model fit by adding or removing predictors based on Akaike Information Criterion (AIC) statistics. In this step, optimal meteorological parameters were selected and used to establish an MLR model. The optimal meteorological parameters, calculated intercept (β_o), regression coefficient ($\beta_{s,c}$), and adjusted R-squared for Jakarta (2013–2019) and Bogor (2017–2019) in the dry, wet, and all seasons are listed in Table 2, and Supplementary Table S3, S4. The MDA8 O_3 resulting from the stepwise MLR model shows the contribution of the meteorological component (MDA8_{met}). The difference between MDA8_{obs} and MDA8_{met} is called the residual and is considered an anthropogenic driver attributed to the ozone variability (MDA8_{ant})[9,10,29].

The total change in meteorological contribution (ΔMDA8_{met}) to O_3 concentration can be calculated as follows:

$$\Delta MDA8_{met} = \sum_{k=1}^{n} \beta_{s,c} x \Delta Met_k \tag{2}$$

where ΔMet_k is the change in the k-th meteorological variable. The change in MDA8_{ant} (ΔMDA8_{ant}) was the difference between the change in observed MDA8 (ΔMDA8_{obs}) and ΔMDA8_{met}. Thus, the relative contribution of meteorology to the ozone concentration could be calculated as the ratio of ΔMDA8_{met} to the total meteorological and anthropogenic factors (ΔMDA8_{met} + ΔMDA8_{ant}).

Ozone formation sensitivity (OFS)

A common approach involves using satellite measurements to determine observed VOC-to-NO_X ratios (FNR). FNRs have been widely used to study OFS. The tropospheric NO_2 column reflects NO_X emissions at the surface because most NO_2 satellite measurements are within the planetary boundary layer and quickly transform or are removed from the atmosphere (short lifetime)[14,18]. HCHO is an intermediate product of all VOCs, and can be used as a proxy for VOC reactivity[54]. HCHO is a short-lived molecule that is usually found near emission sources.

The FNR threshold for separating the VOC-sensitive regime from the NO_x-sensitive regime was derived using various methods for urban areas in the U.S. and China. The FNR threshold can vary by location owing to the influence of precursor emissions, meteorology, and geography[17,55]. This study compared FNR values in Jakarta and Bogor with those reported in the previous studies. The flowchart and methodology used in this study are shown in Supplementary Fig. S11.

Data availability

This study used the products of OMI NO_2 and HCHO from NASA (USA) and European Commission Project for Quality Assurance for Essential Climate Variables (QA4ECV). Meteorological data are available from BMKG (Indonesia) and ECMWF ERA5. Ground O_3 and NO_2 data belong to Jakarta Environmental Agency.

References

1. Lu, H., Lyu, X., Cheng, H., Ling, Z. & Guo, H. Overview on the spatial-temporal characteristics of the ozone formation regime in China. *Environ. Sci. Process. Impacts* **21**, 916–929 (2019).
2. Sillman, S. The relation between ozone, NO(x) and hydrocarbons in urban and polluted rural environments. *Atmos. Environ.* **33**, 1821–1845. https://doi.org/10.1016/S1352-2310(98)00345-8 (1999).
3. Latif, M. T., Huey, L. S. & Juneng, L. Variations of surface ozone concentration across the Klang Valley Malaysia. *Atmos. Environ.* **61**, 434–445. https://doi.org/10.1016/j.atmosenv.2012.07.062 (2012).
4. Mousavinezhad, S., Choi, Y., Pouyaei, A., Ghahremanloo, M. & Nelson, D. L. A comprehensive investigation of surface ozone pollution in China, 2015–2019: Separating the contributions from meteorology and precursor emissions. *Atmos. Res.* **257**, 2015–2019. https://doi.org/10.1016/j.atmosres.2021.105599 (2021).
5. Sharma, S., Sharma, P. & Khare, M. Photo-chemical transport modelling of tropospheric ozone: A review. *Atmos. Environ.* **159**, 34–54. https://doi.org/10.1016/j.atmosenv.2017.03.047 (2017).
6. Chen, Y. *et al.* Relationships of ozone formation sensitivity with precursors emissions, meteorology and land use types, in Guangdong-Hong Kong-Macao Greater Bay Area China. *J. Environ. Sci. (China)* **94**, 1–13. https://doi.org/10.1016/j.jes.2020.04.005 (2020).
7. Dang, R., Liao, H. & Fu, Y. Quantifying the anthropogenic and meteorological influences on summertime surface ozone in China over 2012–2017. *Sci. Total Environ.* **754**, 142394. https://doi.org/10.1016/j.scitotenv.2020.142394 (2021).
8. Inoue, K., Tonokura, K. & Yamada, H. Modeling study on the spatial variation of the sensitivity of photochemical ozone concentrations and population exposure to VOC emission reductions in Japan. *Air Qual. Atmos. Heal.* **12**, 1035–1047. https://doi.org/10.1007/s11869-019-00720-w (2019).
9. Zhang, X. *et al.* First long-term surface ozone variations at an agricultural site in the North China Plain: Evolution under changing meteorology and emissions. *Sci. Total Environ.* **860**, 160520. https://doi.org/10.1016/j.scitotenv.2022.160520 (2023).
10. Li, K. *et al.* Anthropogenic drivers of 2013–2017 trends in summer surface ozone in China. *Proc. Natl. Acad. Sci. U. S. A.* **116**, 422–427. https://doi.org/10.1073/pnas.1812168116 (2019).
11. Jin, X. & Holloway, T. Spatial and temporal variability of ozone sensitivity over China observed from the Ozone Monitoring Instrument. *J. Geophys. Res. Atmos.* **120**, 7229–7246. https://doi.org/10.1002/2015JD023250 (2015).
12. Santiago, J., Inoue, K. & Tonokura, K. Diagnosis of ozone formation sensitivity in the Mexico City Metropolitan Area using HCHO/NO_2 column ratios from the ozone monitoring instrument. *Environ. Adv.* **6**, 100138. https://doi.org/10.1016/j.envadv.2021.100138 (2021).
13. Lee, H. J. *et al.* Satellite-based diagnosis and numerical verification of ozone formation regimes over nine megacities in East Asia. *Remote Sens.* **14**, 1285. https://doi.org/10.3390/rs14051285 (2022).
14. Duncan, B. N. *et al.* Application of OMI observations to a space-based indicator of NOx and VOC controls on surface ozone formation. *Atmos. Environ.* **44**, 2213–2223. https://doi.org/10.1016/j.atmosenv.2010.03.010 (2010).
15. Martin, R. V., Fiore, A. M. & Van Donkelaar, A. Space-based diagnosis of surface ozone sensitivity to anthropogenic emissions. *Geophys. Res. Lett.* **31**, 2–5. https://doi.org/10.1029/2004gl019416 (2004).
16. Tonnesen, G. S. & Dennis, R. L. Analysis of radical propagation efficiency to assess ozone sensitivity to hydrocarbons and NOx 1 Local indicators of instantaneous odd oxygen production sensitivity. *J. Geophys. Res. Atmos.* **105**, 9213–9225. https://doi.org/10.1029/1999JD900371 (2000).
17. Jin, X., Fiore, A., Boersma, K., De Smedt, I. & Valin, L. Inferring Changes in Summertime Surface Ozone–NOx–VOC Jin 2020. pdf. *Environ. Sci. Technol.* **54**, 6518–6529. https://doi.org/10.1021/acs.est.9b07785 (2020).
18. Wang, W., Van Der Ronald, R., Ding, J., Van Weele, M. & Cheng, T. Spatial and temporal changes of the ozone sensitivity in China based on satellite and ground-based observations. *Atmos. Chem. Phys.* **21**, 7253–7269. https://doi.org/10.5194/acp-21-7253-2021 (2021).
19. Fujiwara, M. *et al.* Seasonal variation of tropospheric ozone in Indonesia revealed by 5-year ground-based observations. *J. Geophys. Res. Atmos.* **105**, 1879–1888. https://doi.org/10.1029/1999JD900916 (2000).
20. Komala, N., Saraspriya, S., Kita, K. & Ogawa, T. Tropospheric ozone behavior observed in Indonesia. *Atmos. Environ.* **30**, 1851–1856. https://doi.org/10.1016/1352-2310(95)00382-7 (1996).
21. Wasiah, N. R. & Driejana, D. Modelling of tropospheric ozone concentration in urban environment. *IPTEK J. Proc. Ser.* https://doi.org/10.12962/j23546026.y2017i6.3279 (2017).
22. Santoso, M. *et al.* Long term characteristics of atmospheric particulate matter and compositions in Jakarta Indonesia. *Atmos. Pollut. Res.* https://doi.org/10.1016/j.apr.2020.09.006 (2020).
23. Verma, R. L. *et al.* Air quality management status and needs of countries in South Asia and Southeast Asia. *APN Sci. Bull.* **13**, 102. https://doi.org/10.30852/sb.2023.2222 (2023).
24. Sun, J. *et al.* Long-term variations of meteorological and precursor influences on ground ozone concentrations in Jinan, North China Plain, from 2010 to 2020. *Atmosphere (Basel).* **13**, 994. https://doi.org/10.3390/atmos13060994 (2022).
25. Tao, M. *et al.* Investigating changes in ozone formation chemistry during summertime pollution events over the Northeastern United States. *Environ. Sci. Technol.* **56**, 15312–15327. https://doi.org/10.1021/acs.est.2c02972 (2022).

26. Kusumaningtyas, S. D. A., Khoir, A. N., Fibriantika, E. & Heriyanto, E. Effect of meteorological parameter to variability of Particulate Matter (PM) concentration in urban Jakarta city, Indonesia. *IOP Conf. Ser. Earth Environ. Sci.* **724**, 012050. https://doi.org/10.1088/1755-1315/724/1/012050 (2021).

27. Permadi, D. A. & Kim Oanh, N. T. Episodic ozone air quality in Jakarta in relation to meteorological conditions. *Atmos. Environ.* **42**, 6806–6815. https://doi.org/10.1016/j.atmosenv.2008.05.014 (2008).

28. Ning, G. *et al.* Impact of low-pressure systems on winter heavy air pollution in the northwest Sichuan Basin China. *Atmos. Chem. Phys.* **18**, 13601–13615. https://doi.org/10.5194/acp-18-13601-2018 (2018).

29. Chen, L., Zhu, J., Liao, H., Yang, Y. & Yue, X. Meteorological influences on PM2.5 and O3 trends and associated health burden since China's clean air actions. *Sci. Total Environ.* **744**, 140837. https://doi.org/10.1016/j.scitotenv.2020.140837 (2020).

30. He, J. *et al.* Air pollution characteristics and their relation to meteorological conditions during 2014–2015 in major Chinese cities. *Environ. Pollut.* **223**, 484–496. https://doi.org/10.1016/j.envpol.2017.01.050 (2017).

31. Ou-Yang, C. F. *et al.* Detection of stratospheric intrusion events and their role in ozone enhancement at a mountain background site in sub-tropical East Asia. *Atmos. Environ.* **268**, 118779. https://doi.org/10.1016/j.atmosenv.2021.118779 (2022).

32. Vohra, K. *et al.* Long-Term trends in air quality in major cities in the UK and India: A view from space. *Atmos. Chem. Phys.* **21**, 6275–6296. https://doi.org/10.5194/acp-21-6275-2021 (2021).

33. Itahashi, S., Irie, H., Shimadera, H. & Chatani, S. fifteen-year trends (2005–2019) in the satellite-derived ozone-sensitive regime in east Asia: A gradual shift from VOC-sensitive to NOx-sensitive. *Remote Sens.* **14**, 4512. https://doi.org/10.3390/rs14184512 (2022).

34. Agustian Permadi, D., Dirgawati, M., Ghani Kramawijaya, A. & Hermawan, W. Preliminary estimation on air pollution load over Bogor city towards development of clean air action plan. *J. Ecolab* **14**, 53–62. https://doi.org/10.20886/jklh.2020.14.1.53-62 (2020).

35. Lestari, P., Arrohman, M. K., Damayanti, S. & Klimont, Z. Emissions and spatial distribution of air pollutants from anthropogenic sources in Jakarta. *Atmos. Pollut. Res.* **13**, 101521. https://doi.org/10.1016/j.apr.2022.101521 (2022).

36. Sofyan, A., Toshihiro, K. & Kurata, G. Difference of sea breeze in Jakarta between dry and wet seasons: Implication in NO₂ and SO₂ distribution in Jakarta. *J. Glob. Environ. Eng.* **12**, 63–85 (2007).

37. Kitada, T., Sofyan, A. & Kurata, G. Numerical simulation of air pollution transport under sea/land breeze situation in Jakarta, Indonesia in dry season. In *Air Pollution Modeling and its Application XIX* (eds Borrego, C. & Miranda, A. I.) 243–251 (Springer Netherlands, Dordrecht, 2008). https://doi.org/10.1007/978-1-4020-8453-9_27.

38. Syahdiza, R., Dewi, S., Halidah, H., Belgaman, H. A. & Renggono, F. Sea breeze observation in bogor based on 2016 intensive observation period (IOP). *AGERS 2019 - 2nd IEEE Asia-Pacific Conf. Geosci. Electron. Remote Sens. Technol. Underst. Forecast. Dyn. Land, Ocean Marit. Proceeding* 6–9 (2019) https://doi.org/10.1109/AGERS48446.2019.9034344.

39. Myllyvirta, L., Suarez, I., Uusivuori, E. & Thieriot, H. *Transboundary Air Pollution in the Jakarta , Banten , and West Java provinces.* (2020).

40. Permadi, D. A., Sofyan, A. & Kim Oanh, N. T. Assessment of emissions of greenhouse gases and air pollutants in Indonesia and impacts of national policy for elimination of kerosene use in cooking. *Atmos. Environ.* **154**, 82–94. https://doi.org/10.1016/j.atmosenv.2017.01.041 (2017).

41. National Statistical Agency (BPS). *Number of Motorized Vehicles by Type of Vehicle (unit) in DKI Jakarta Province.* https://jakarta.bps.go.id/indicator/17/786/1/jumlah-kendaraan-bermotor-menurut-jenis-kendaraan-unit-di-provinsi-dki-jakarta.html.

42. Hien, T. T. *et al.* Comprehensive volatile organic compound measurements and their implications for ground-level ozone formation in the two main urban areas of Vietnam. *Atmos. Environ.* **269**, 118872. https://doi.org/10.1016/j.atmosenv.2021.118872 (2022).

43. Yudison, A. P. & Driejana, D. Determination of Btex concentration using passive samplers in a heavy traffic area of Jakarta. *Indonesia. Int. J. Geomate* **19**, 180–187. https://doi.org/10.21660/2020.76.97945 (2020).

44. Vazquez Santiago, J., Sosa Echeverria, R., Garza Galindo, R. & Fuentes Garcia, G. Spatiotemporal variations in the air concentrations of 1,3-butadiene in intra-urban environments: a case study in southern Mexico City. *Int. J. Environ. Sci. Technol.* **20**, 9441–9450. https://doi.org/10.1007/s13762-022-04639-1 (2023).

45. Zulkifli, M. F. H. *et al.* Volatile organic compounds and their contribution to ground-level ozone formation in a tropical urban environment. *Chemosphere* **302**, 134852. https://doi.org/10.1016/j.chemosphere.2022.134852 (2022).

46. Kusumaningtyas, S. D. A., Aldrian, E., Wati, T., Atmoko, D. & Sunaryo,. The recent state of ambient air quality in Jakarta. *Aerosol Air Qual. Res.* **18**, 2343–2354. https://doi.org/10.4209/aaqr.2017.10.0391 (2018).

47. National Statistical Agency (BPS). Number of Motorized Vehicles by Type of Vehicle (unit) in DKI Jakarta Province. https://jakarta.bps.go.id/indicator/17/786/1/jumlah-kendaraan-bermotor-menurut-jenis-kendaraan-unit-di-provinsi-dki-jakarta.html (2022).

48. Ren, J., Hao, Y., Simayi, M., Shi, Y. & Xie, S. Spatiotemporal variation of surface ozone and its causes in Beijing, China since 2014. *Atmos. Environ.* **260**, 118556. https://doi.org/10.1016/j.atmosenv.2021.118556 (2021).

49. Nishihashi, M. *et al.* Greenhouse gases and air pollutants monitoring project around Jakarta megacity. *IOP Conf. Ser. Earth Environ. Sci.* **303**, 012038. https://doi.org/10.1088/1755-1315/303/1/012038 (2019).

50. Levelt, P. F. *et al.* The ozone monitoring instrument. *IEEE Trans. Geosci. Remote Sens.* **44**, 1093–1100. https://doi.org/10.1109/TGRS.2006.872333 (2006).

51. Lefohn, A. S. *et al.* Tropospheric ozone assessment report: Global ozone metrics for climate change, human health, and crop/ecosystem research. *Elementa* https://doi.org/10.1525/elementa.279 (2018).

52. Chang, K. L. *et al.* Trend detection of atmospheric time series: Incorporating appropriate uncertainty estimates and handling extreme events. *Elementa* **9**, 1–28. https://doi.org/10.1525/elementa.2021.00035 (2021).

53. Cooper, O. R. *et al.* Multi-decadal surface ozone trends at globally distributed remote locations. *Elementa* https://doi.org/10.1525/elementa.420 (2020).

54. Sillman, S. The use of NOy, H2O2, and HNO3 as indicators for ozone-NOx-hydrocarbon sensitivity in urban locations. *J. Geophys. Res.* **100**, 175–188 (1995).

55. Chen, Y. *et al.* Research on the ozone formation sensitivity indicator of four urban agglomerations of China using Ozone Monitoring Instrument (OMI) satellite data and ground-based measurements. *Sci. Total Environ.* **869**, 161679. https://doi.org/10.1016/j.scitotenv.2023.161679 (2023).

Acknowledgements

Author contributions

S.D.A.K.: formal analysis, investigation, analyzed the data, and wrote the paper. K.T.: conceptualization, methodology, supervision, wrote and reviewed the final draft. R.M.: wrote codes, performed software, and produced Fig. 2, 4, 6. D.G., A.S.: reviewed and edited the paper. R.R., N.S.: responsible for air quality data. W.I.: data curation, reviewed, and edited. P.L., and D.A.P.: performed data curation.

Competing interests

The authors declare no competing interests.

Additional information

Supplementary Information The online version contains supplementary material available at https://doi.org/10.1038/s41598-024-60374-2.

Correspondence and requests for materials should be addressed to S.D.A.K. or K.T.

Reprints and permissions information is available at www.nature.com/reprints.

Publisher's note Springer Nature remains neutral with regard to jurisdictional claims in published maps and institutional affiliations.